

Dynamics of Turing patterns under spatio-temporal forcing

S. Rüdiger^{1,2}, D. G. Míguez³, A. P. Muñuzuri³, F. Sagués⁴ and J. Casademunt¹

¹*Dept. E.C.M., Facultat de Física, Universitat de Barcelona, Av. Diagonal 647, 08028 Barcelona, Spain*

²*School of Computational Science and Information Technology, F.S.U, Tallahassee FL 32306, USA*

³*Facultade de Física, Universidade de Santiago de Compostela, 15782 Santiago de Compostela, Spain and*

⁴*Departament de Química Física, Universitat de Barcelona, Martí i Franquès 1, 08028 Barcelona, Spain*

We study, both theoretically and experimentally, the dynamical response of Turing patterns to a spatio-temporal forcing in the form of a travelling wave modulation of a control parameter. We show that from strictly spatial resonance, it is possible to induce new, generic dynamical behaviors, including temporally-modulated travelling waves and localized travelling soliton-like solutions. The latter make contact with the soliton solutions of P. Coulet *Phys. Rev. Lett.* **56**, 724 (1986) and provide a general framework which includes them. The stability diagram for the different propagating modes in the Lengyel-Epstein model is determined numerically. Direct observations of the predicted solutions in experiments carried out with light modulations in the photosensitive CDIMA reaction are also reported.

PACS numbers: 82.40.Ck, 47.54.+r, 82.40.Bj, 47.20.Ky

The study of pattern dynamics under external forcing provides a powerful tool to deeply probe their inherently nonlinear mechanisms under non-equilibrium conditions. A great deal of attention has been focused on resonances or locking of spatially structured states, either stationary or oscillatory, under temporal (spatially uniform) [1, 2, 3, 4, 5] or spatial (steady) modulations [6, 7, 8, 9, 10]. Steady patterns in reaction-diffusion systems typically arise from the celebrated Turing mechanism [11, 12]. According to it, inhomogeneous distributions of chemical concentrations self-organize spontaneously out of a non-structured medium as a result of a competition between autocatalytic reaction steps and the differential diffusivities of an activator (smaller) and an inhibitor-like (larger diffusion) species. Turing patterns are endowed with an intrinsic wavelength, depending only on the kinetic and diffusion parameters, but lack an intrinsic frequency, in contrast to oscillatory chemical systems [12]. Genuine Turing patterns were first observed in quasi two-dimensional gel reactors (pre-loaded with appropriate chemical indicators) in the CIMA [13] and the CDIMA [14] reactions, and appear as patterned distributions of iodide. The CDIMA reaction has the interesting feature of being photosensitive [15].

It seems thus timely to search for generic behavior in the unexplored perspective of spatio-temporal forcing of pattern forming systems. Specifically, we aim at studying the dynamical response of photosensitive Turing patterns to the simplest external spatio-temporal forcing consisting of a travelling-wave modulation of the control parameter associated to the illumination. Through the mechanism of pure spatial resonance an external frequency will thus be imposed in an otherwise nonoscillatory system. As a consequence, new nontrivial dynamical modes are expected to arise which allow to connect the two trivial limiting cases, namely: a travelling pattern locked to the forcing at low velocities and a standing pattern resulting

from the time-averaging of the forcing at large velocities. Analytical and numerical results will be reported featuring the simplest of these spatio-temporal behaviors. Experiments conducted with the CDIMA reaction are also provided which fully confirm our theoretical predictions. Beyond the particular chemical context that motivates our study, such solutions, and the conditions of their appearance, are sufficiently generic to be applicable to a rather general class of pattern forming systems including for instance Rayleigh-Bénard convection. In a sense, our study may be viewed as a development of the work of Coulet [7, 16] on commensurate-incommensurate transitions in nonequilibrium (spatially) forced systems.

The experimental system under study is modelled within the Lengyel-Epstein scheme [14], once modified to include the effect of illumination, as [15]:

$$\partial_t u = a - cu - 4 \frac{uv}{1+u^2} - \phi + \frac{\partial^2 u}{\partial x^2}, \quad (1)$$

$$\partial_t v = \sigma(cu - \frac{uv}{1+u^2} + \phi + d \frac{\partial^2 v}{\partial x^2}). \quad (2)$$

Here u and v are the dimensionless concentrations of two of the chemical species; a , c , σ , and d denote dimensionless parameters of the chemical system. The effect of external illumination is introduced through the ϕ -terms. This contribution can be decomposed into the mean value ϕ_0 and a modulation part: $\phi(x, t) = \phi_0 + \epsilon \cos(k_f x + \omega t)$. For purely homogeneous illumination, $\epsilon = 0$, the equations admit a solution which in the following will be referred to as base state: $u_0 = (a - 5\phi_0)/(5c)$, $v_0 = a(1 + u_0^2)/(5u_0)$.

All our numerical results are obtained through integration of the model reaction-diffusion equations (1),(2) with periodic boundary conditions by means of a pseudo-spectral method with a linear-implicit time-stepping. From here on we fix the parameters to the following: $a = 16$, $c = 0.6$, $d = 1.07$, and $\sigma = 301$. These values

were chosen to reproduce the experimental conditions referred to below. The large σ value, corresponding to a strong diffusion contrast between the two species, guarantees that we are far from the oscillatory regime of this chemical system. Consequently, only the Turing bifurcation will play a role. The remaining parameters concern the forcing term. One of them, ϕ_0 , will serve as the parameter to locate the position of the Turing bifurcation in the homogeneous problem. For the given parameters it occurs at $\phi_0 \approx 2.3$ (the base state being unstable to Turing patterns below $\phi_0 \approx 2.3$) and the critical wavenumber is $k_c \approx 1.07$.

We begin our analysis with the case of exact 1:1 spatial resonance $k_c = k_f$. Choosing the length L of the periodic domain to be 10λ , where $\lambda = 2\pi/k_c$ is the critical wavelength at instability, we fix $L = 58.72$ and the amplitude $\epsilon = 0.1$.

As is known from the analysis of time-independent forcing, the spatial 1:1 resonance yields an imperfect bifurcation to Turing patterns [7]. Accordingly, the base state ceases to be a stationary solution and is modified into a non-homogeneous state for every value of the bifurcation parameter ϕ_0 . For ϕ_0 in the stable region (above 2.3) this state is a travelling wave (TW). The TW locks to the forcing wave, adopting the same wave-number and frequency, with only a constant phase difference. This is the trivial state to be expected for slow driving. For large ω the amplitude of the TW approaches 0. The TW's exist to the right of the solid curve in fig. 1.

Crossing the solid curve in fig. 1 the TW state undergoes a first instability into a state with temporally modulated amplitude (MTW, triangles in fig. 1). This is the signature of a Hopf bifurcation which introduces a new frequency f_H (see fig. 2a). Note that the modulation of the amplitude occurs uniformly in the entire system. We found that for large ω the Hopf frequency converges to the frequency ω of the forcing wave.

The solutions and the transition described above can be rationalized in terms of an amplitude equation. Following standard envelope techniques near threshold [7, 17], and with the forcing being invariant under the transformation $t \rightarrow t+T$, $x \rightarrow x-\omega T/k_f$, for sufficiently small ϵ and ω , the slowly varying modulations of the travelling mode, in the case of perfect 1:1 resonance ($k_f = k_c$) will be given by the amplitude equation

$$\dot{A} = \mu A - |A|^2 A + \epsilon \exp(-i\omega t) + \partial^2 A / \partial x^2. \quad (3)$$

Using polar coordinates, $A = R \exp i\Theta$, we look for homogeneous solutions with $\Theta = \Theta_0 - \omega t$. As in the steady case for $\epsilon \neq 0$ there is a non-zero solution for every μ , the dimensionless distance to threshold. Its amplitude approaches 0 with increasing ω in accordance with our observations for the Lengyel-Epstein model. Θ_0 is the phase shift between the forcing wave and the resulting pattern.

We further determine the stability of this solution with respect to homogeneous perturbations. Directly from the amplitude equation:

$$\dot{R} = \mu R - R^3 + \epsilon \cos(\psi + \Theta_0), \quad (4)$$

$$\dot{\psi} = -\frac{\epsilon}{R} \sin(\psi + \Theta_0) + \omega, \quad (5)$$

where we have defined: $\psi = \Theta + \omega t - \Theta_0$. Linearization about the locked solution ($\psi = 0$, $R = Q = \text{const}$) yields the following eigenvalues: $\lambda = \mu - 2Q^2 \pm \sqrt{(Q^4 - \omega^2)}$. Corresponding to fig. 1, for large ω , the marginal curve approaches the line $\mu = 0$, and the imaginary part of the eigenvalue, converges to the driving frequency, as also observed numerically above [18].

We now address the more generic case of inexact 1:1 resonance [19], introducing a slight wavenumber misfit, $k_f \neq k_c$. To allow for a continuous variation of the misfit in a finite system, we will fix the integer wavenumber ($n = kL/2\pi$) of the forcing to $n = 10$ and change smoothly the length L of the periodic domain. For example, for $L = 65$ the 10th wave number corresponds to $k_f \approx 0.97$. Fig. 3 depicts the complex behavior that was found changing k_f from 0.9 to 1.26 ($L = 70, \dots, 50$). The average illumination ϕ_0 was fixed to 2.25 during all of the simulations. For the purely homogeneous forcing (i.e. $\phi' = 0$) this value corresponds to a slightly unstable base state.

In fig. 3 the stability domain in ω and k_f is given for four different states. The TW state, the solution locked to the forcing, is the only stable solution for approximately $\omega \leq 1$. Above a roughly horizontal transition curve close to $\omega = 1.1$ the TW states are unstable. For $k_f = k_c$ and close to this point the transition occurs at $\omega \approx 1.15$ (cf. fig. 1) and results in the MTW.

The domain of stability of the MTW is given by the solid curve in fig. 3. Outside of this domain the attractors are either the TW state or one of two different new localized states which we call soliton waves (SOW)[20]. A typical space-time plot is shown in fig. 2b. Spatial plots of these states show that they resemble the soliton-like solutions for the case of non-travelling forcing [7] but they exhibit the following new properties: the soliton, i.e., the localized suppression of the amplitude moves relatively to the underlying travelling pattern with a relative velocity which may be positive or negative. Furthermore, as the soliton travels along the pattern the phase of the background pattern moves in either direction. In our case the integer wavenumber of the background pattern is either $n = 9$ or $n = 11$ and the corresponding states are represented in fig. 3 with circles and diamonds, respectively.

Beyond the range of forcing wavenumbers shown in fig. 3 there exist further soliton states in accordance with the prediction for non-travelling forcing [7]. Here we will describe only the two states that are adjacent to the MTW state in fig. 3. The states represented by diamonds (resp. circles) carry a soliton that moves to the

right (resp. left). The approximate range of stability for these states is given by the dashed curve (resp. dotted curve).

Note that the stability domains of the soliton states and the MTW state overlap. Remarkably, at sufficiently large ω the soliton states are even stable for $k_f = k_c$, i.e., exact 1:1 resonance. This contrasts to the case of static forcing [7] where only the presence of a misfit can lead to solitons.

The above localized states (SOW) can be described as quasi-periodic in the sense that their behavior can be reproduced as superposition of two modes, namely, the forcing (travelling) mode with wavelength $L/10$ and an adjacent mode with wavelength $L/9$ or $L/11$, typically the closer one to the characteristic wavelength of the Turing instability. The excited Turing mode is standing so that the superposition of both yields a localized envelope (soliton) moving to the right ($L/11$) or to the left ($L/9$). Furthermore, one finds the velocity of the soliton to be proportional to the quotient of ω and the difference of the wavenumbers of the two modes, which agrees with numerical results of the full problem.

Note that the phase diagram depicted in fig. 3 exhibits large regions of multistability, with the corresponding hysteresis. It is worth remarking that the stability boundaries here reported may well be affected by to finite-size effects, since possible long wave-length, phase instabilities may be prevented by the finite size of our simulations. A full envelope and phase-diffusion description of this scenario in an infinite system deserves a detailed study and will be addressed elsewhere.

A link between the SOW's and the solitons for steady forcing is apparent for smaller ϵ . We decreased the value of ϵ to 0.003 and determined the domain of stability for the soliton 11 state for ω values close to 0 (fig. 4). It appears that even for vanishing ω the soliton states persist and the domain of stability forms a "tongue" with a finite range at $\omega = 0$. For larger ϵ and $\omega = 0$ the SOW's do not exist since the driving term dominates the equations and forces a homogeneous pattern. Therefore it seems that the relative suppression of the forcing term by a effective time-averaging due to a fast travelling forcing may account for the existence of soliton states for larger ϵ .

To prove the feasibility of controlled spatio-temporal forcing and to check the validity and robustness of our predictions in a real system undergoing a Turing instability, we have carried out experiments on the (photosensitive) CDIMA chemical reaction, using the projection of travelling light patterns as the controlled forcing. Experiments were performed in a thermostated continuously fed unstirred one-feeding-chamber reactor at 4 ± 0.5 C. Structures appear in an agarose gel layer (2% agarose, thickness 0.3 mm, diameter 20 mm). The gel layer was separated from the feeding chamber by an Anapore membrane (Whatman, pore size 0.2 mm) and a nitrocellulose membrane (Schleicher & Schnell, pore size 0.45 mm).

Under the chosen set of reagent concentrations (see caption of fig.5), the system at dark spontaneously yields disordered stripe patterns with a wavelength of 0.54 mm. In a typical experiment, parallel light stripes with a characteristic wavelength of precisely 0.54 mm were focused on the gel layer and were moved in the horizontal direction with well-controlled and constant velocity v . For very small values, trivial travelling stripes, following adiabatically the imposed pattern, were found, as expected. As the passing velocity was increased they readily transformed into the modulated striped mode, as predicted by the theory (see fig. 5a). Furthermore, when considering a slight misfit (see caption of fig.5), a localized structure was observed, propagating in the opposite direction to that of the stripes (see fig. 5b). This again constitutes a neat confirmation of our theoretical findings. Further experiments are presently being conducted to look for other modes of dynamical responses to such a spatio-temporal modulation and will be published elsewhere.

We have described a generic mechanism to induce new pattern dynamics through spatial resonance. The phenomenon is claimed to be generic for systems undergoing a Turing instability. For instance we have already observed the same type of response in the 1d Swift-Hohenberg equation. Within the framework of chemical Turing patterns, the consideration of the 2d case is readily accessible and points out to even richer phenomena.

S.R. is supported by the NSF under contract DMR-0100903. Financial support from DGI (Spain) under projects BXX2000-0638-C02 and BFM2000-0348, and also from European Commission under network HPRN-CT-2002-00312 is acknowledged.

-
- [1] V. Petrov, Q. Ouyang, and H. L. Swinney, *Nature* **388**, 655 (1997).
 - [2] A. L. Lin, A. Hagberg, A. Ardelea, M. Bertram, H. L. Swinney, and E. Meron, *Phys. Rev. E* **62**, 3790 (2000).
 - [3] V.K. Vanag, A.M. Zhabotinsky, and I.R. Epstein, *Phys. Rev. Lett.* **86**, 552 (2001).
 - [4] A. Careta and F. Sagués, *J. Chem. Phys.* **92**, 1098 (1990).
 - [5] A. K. Horvath, M. Dolnik, A.P. Muñuzuri, A.M. Zhabotinsky, and I.R. Epstein, *Phys. Rev. Lett.* **83**, 2950 (1999); M. Dolnik, A.M. Zhabotinsky, and I.R. Epstein, *Phys. Rev. E* **63**, 026101 (2001).
 - [6] M. Lowe, J. Gollub, and J.L. Lubensky, *Phys. Rev. Lett.* **51**, 786 (1983); M. Lowe and J. Gollub, *Phys. Rev. A* **31**, 3893 (1985).
 - [7] P. Coulet, *Phys. Rev. Lett.* **56**, 724 (1986).
 - [8] P. Coulet and D. Walgraef, *Europhys. Lett.* **10**, 525 (1989).
 - [9] J.P. Voroney, A.T. Lawniczak, and R. Kapral, *Physica D* **99**, 303 (1996).
 - [10] M. Dolnik, I. Berenstein, A.M. Zhabotinsky, and I.R. Epstein, *Phys. Rev. Lett.* **87**, 238301 (2001).
 - [11] A.M. Turing, *Philos. Trans. Roy. Soc. London, Ser B* **237**, 37 (1952)

- [12] *Chemical Waves and Patterns*, R. Kapral and K. Showalter Eds., Kluwer Acad. Publ, Dordrecht (1995).
- [13] V. Castets, E. Dulos, J. Boissonade, and P. De Kepper, Phys. Rev. Lett. **64**, 2953 (1990); Q. Ouyang and H.L. Swinney, Nature **352**, 610 (1991).
- [14] I. Lengyel and I. R. Epstein, Science **251**, 650 (1991).
- [15] A. P. Muñuzuri, M. Dolnik, A. M. Zhabotinsky, and I. R. Epstein, J. Am. Chem. Soc. **121**, 8065 (1999).
- [16] P. Coullet and P. Huerre, Physica D **23**, 27 (1986)
- [17] M. Cross, P. Hohenberg, Rev. Mod. Phys. **65**, 851 (1993)
- [18] Further analysis shows that this instability is related to the loss of a stable fixed-point solution in the homogeneous phase diffusion equation (5).
- [19] We have also observed the transition from TW to MTW at 2:1 resonance.
- [20] The term 'soliton' is abused here in the sense of localized modulation, but the referred states are not necessarily solitons in a strict sense.

FIG. 1: Type of attractor for different values of ω and average illumination ϕ_0 : boxes correspond to TW solutions, triangles to MTW solutions (see text). The vertical line shows the position of the instability for homogeneous forcing.

FIG. 2: Space-time plots of the u -component of the modulated travelling wave solution for $\omega = 0.5$ and $\phi_0 = 2.11$ (a); and for the soliton solution for $\omega = 5$, $\phi_0 = 2.25$ and $k_f = 0.9$ (b).

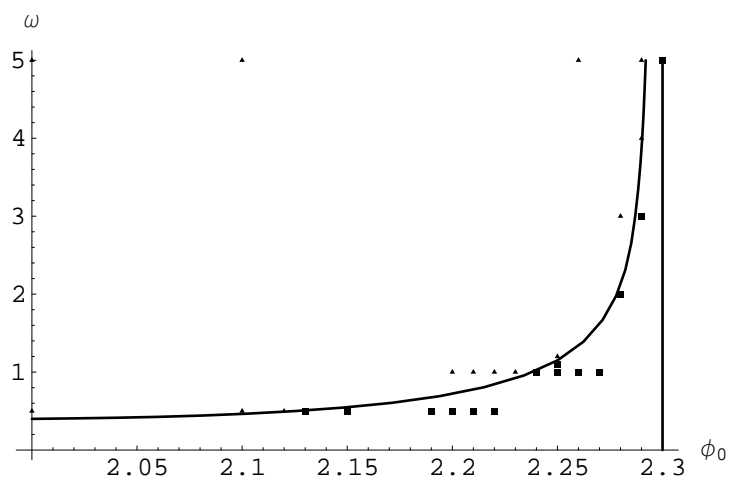
FIG. 3: Phase diagram in the space of ω (vertical) and k_f (horizontal), filled box - TW, filled triangle - MTW (see text for notation), diamond - soliton state with wave length $L/11$, circle - soliton state with wave length $L/9$. We have chosen $\phi_0 = 2.25$. The value $k_f = k_c$ ($L = 58.72$) corresponds to the dashed vertical line showing the position of the perfect 1:1 resonance.

FIG. 4: 'Tongue' of soliton states as a function of ω for small ϵ . The dashed line approximates the boundary of the soliton 'tongue' with $n = 11$ as it approaches the $\omega = 0$ line (spatial forcing of Ref.[7]). Here we have used $\epsilon = 0.003$.

FIG. 5: Experimental space-time plots for the modulated travelling wave solution (a) and for the soliton solution (b). The dashed line in (b) is a guide to the eye. The input concentrations of reagents are 0.45 mM I₂, 0.078 mM ClO₂, 10 mM H₂SO₄, 1.2 mM malonic acid and 10 mM polyvinil alcohol with a residence time in the reactor of 250 s. With these parameters the system spontaneously yields stripe patterns with a wavelength of 0.54 mm. (Experimental parameters: $v = 0.13$ mm/h for both cases, the imposed wavelength is 1.1 times the spontaneous one in the case of the soliton solution case).

This figure "fig2.png" is available in "png" format from:

<http://arxiv.org/ps/physics/0301079v1>



This figure "fig5.png" is available in "png" format from:

<http://arxiv.org/ps/physics/0301079v1>

